Genetic and functional adaptations and alcohol-biased signaling in the mediodorsal thalamus of alcohol dependent mice

Jayden C. Martin[1], Kaitlin C. Reeves[1], Kathryn A. Carter[1], Matthew Davis[1], Amelia Schneider[1], Ellie Meade[1], Christina L. Lebonville[2], Sudarat Nimitvilai[1], Michaela Hoffman[2], John J. Woodward[1], Patrick J. Mulholland[1]*, and Jennifer A. Rinker[1]*

[1]Department of Neuroscience, [2]Department of Psychiatry and Behavioral Sciences, Charleston Alcohol Research Center, Medical University of South Carolina

*Co-corresponding authors

Dr. Jennifer A. Rinker
rinker@musc.edu

Dr. Patrick J. Mulholland
mulholl@musc.edu

Abstract

Alcohol Use Disorder (AUD) is a significant health concern characterized by an individual's inability to control alcohol intake. With alcohol misuse increasing and abstinence rates declining, leading to severe social and health consequences, it is crucial to uncover effective treatment strategies for AUD by focusing on understanding neuroadaptations and cellular mechanisms. The mediodorsal thalamus (MD) is a brain region essential for cognitive functioning and reward-guided choices. However, the effects of alcohol (ethanol) dependence on MD neuroadaptations and how dependence alters MD activity during choice behaviors for alcohol and a natural reward (sucrose) are not well understood. Adult C57BL/6J mice treated with chronic intermittent ethanol (CIE) exposure were used to assess genetic and functional adaptations in the MD. Fiber photometry-based recordings of GCaMP6f expressed in the MD of C57BL/6J mice were acquired to investigate in vivo neural adaptations during choice drinking sessions for alcohol (15%) and either water or sucrose (3%). There were time-dependent changes in cFos and transcript expression during acute withdrawal and early abstinence. Differentially expressed genes were identified in control mice across different circadian time points and when comparing control and alcohol dependent mice. Gene Ontology enrichment analysis of the alcohol-sensitive genes revealed disruption of genes that control glial function, axonal myelination, and protein binding. CIE exposure also increased evoked firing in MD cells at 72 hours of withdrawal. In alcohol-dependent male and female mice that show increased alcohol drinking and preference for alcohol over water, we observed an increase in alcohol intake and preference for alcohol when mice were given a choice between alcohol and sucrose. Fiber photometry recordings demonstrated that MD activity is elevated during and after licking bouts for alcohol, water, and sucrose, and the signal for alcohol is significantly higher than that for water or sucrose during drinking. The elevated signal during alcohol bouts persisted in alcohol dependent mice. These findings demonstrate that CIE causes genetic and functional neuroadaptations in the MD and that alcohol dependence enhances alcohol-biased behaviors, with the MD uniquely responsive to alcohol, even in dependent mice.

Introduction

Alcohol Use Disorder (AUD) is characterized by excessive alcohol consumption and the inability to control drinking behavior. Since 1990, binge drinking prevalence has sharply increased, while lifetime abstinence rates have declined[1]. Being the most common substance use disorder globally, AUD affects approximately 8% of the population[2]. Predictions indicate that rates of excessive alcohol consumption will continue to rise over the next decade, further intensifying alcohol-related health issues and diminishing quality of life. Individuals with AUD frequently display poor decision-making and impaired behavioral flexibility, often placing alcohol over other priorities and naturally rewarding behaviors, e.g., work, family, alternative non-drug rewards. Behavioral flexibility—the ability to adjust actions based on changes in reward value—is a critical characteristic of alcohol and substance use disorders[3]. Impaired behavioral flexibility is often associated with mood disorders, anxiety, and psychiatric comorbidities. Individuals with AUD show increased alcohol-approach associations on an implicit association task, and this alcohol-biased behavior is associated with increased lifetime alcohol use and fewer days of abstinence[4]. This biased choice for alcohol has also been modeled in rodents, whereby rodents choose alcohol over social interaction and sweetened solutions[5-8]. Identifying the neural circuits amplifying alcohol's motivational power and improper behavioral flexibility in decision-making driving alcohol dependence is, therefore, essential for developing therapeutic interventions for AUD.

The mediodorsal thalamus (MD) is a crucial region of interest in AUD research due to its role in memory, cognition, and reward-guided behavior[9,10]. The MD and prefrontal cortex (PFC) connectivity influences higher-order cognitive functions, such as reward processing and decision-making. Additionally, the MD functions as both a simple relay structure and a dynamic integrator, stabilizing task-relevant prefrontal activity and facilitating top-down signaling from the PFC[11]. Thalamocortical and corticothalamic loops support adaptive decision-making, behavioral flexibility, and cognitive domains profoundly impacted by AUD. Additionally, the medial and lateral subnuclei of the MD innervate the PFC while exhibiting distinct functional properties. Characteristic properties of the medial subnucleus include longer membrane times and higher action potential frequencies, hinting at differential roles in modulating cortical activity[12]. An analysis of tractography studies revealed overall degeneration of white matter tracts between the MD and PFC[13], potentially disrupting goal-directed behaviors. The disruption between the MD and the PFC may contribute to the impaired behavioral flexibility and increased impulsivity observed in many individuals with AUD. The influence of the MD extends beyond its subcortical and cortical connections, as it innervates and shares connections with brain regions essential for drug-seeking behavior, including the amygdala, ventral tegmental area (VTA), and nucleus accumbens[14]. The reciprocal glutamatergic projections with these brain regions enable the MD to orchestrate complex behaviors like decision-making and behavioral flexibility, both of which are crucial areas in understanding more about alcohol misuse.

Inhibiting or lesioning the mediodorsal thalamus (MD) have provided critical insights into its functional roles, helping to clarify its impact on neural circuits and behavior. Damage to the MD has been shown to disrupt the ability to encode action-outcome associations, one essential for adaptive decision-making. Additionally, MD lesions impaired the updating of reward value, as seen in reinforcer devaluation tasks-experiments that asses how changes in the value of a reward influence choice behavior- although primary preference shifts remain unaffected[3]. In studies with non-human primates, MD lesions resulted in cognitive deficits comparable to those following PFC damage, especially in tasks requiring flexible reward updating and reinforcement devaluation[15,16]. MD lesions also impaired the ability to process odor samples and recognize familiar stimuli[17,18], suggesting a possible connection to goal-directed alcohol-seeking behavior based on sensory cues. Although the MD has been implicated in impaired decision-making and flexible reward updating, both essential factors in understanding AUD, more research is needed to understand how alcohol dependence alters MD activity and how these changes contribute to compulsive alcohol consumption. Triggers for alcohol-seeking behavior have been linked to higher CaMKII activity in the MD, suggesting this brain region's role in the relapse of alcohol drinking[19]. Acute alcohol disrupts local field potential rhythms in the mouse MD, demonstrating its sensitivity to the neurophysiological effects of alcohol[20]. Additionally, long-term damage to the MD and midline thalamic regions has been documented in AUD patients, such as those with Korsakoff's syndrome[13,21]. Mice with physical dependence induced by chronic ethanol exposure show elevated serotonin transporter expression[22]and withdrawal-induced cFos expression in the MD of PKC-ε KO knockout mice[23], suggesting neurological changes in serotonin availability and heightened responsiveness of neurons in the MD in response to chronic alcohol.

While the MD is implicated in impaired decision-making and neurological changes, its specific role in chronic alcohol-induced behavioral deficits remains relatively unexplored.

The current study explores how alcohol dependence induced by chronic intermittent ethanol (CIE) vapor exposure induces genetic and physiological adaptations using Nanostring transcriptomic analyses and slice electrophysiology. Using fiber photometry, real-time calcium dynamics were tracked in the MD, investigating how alcohol dependence affects decision-making between alcohol and non-alcohol options. We propose that CIE exposure will lead to altered function, gene expression, and in vivo calcium signaling in the MD, particularly during alcohol consumption. A deeper understanding of how the MD is influence by and controls excessive alcohol consumption could aid in preventing relapse and improving treatment options for individuals with AUD.

Materials and Methods

Animals

Adult male and female C57BL/6J mice (8-12 weeks old at time of experiment) were obtained from Jackson Laboratories (stock # 000664). Mice were single housed in standard cages with ad libitum access to food and water, unless otherwise indicated, and were housed on a 12-hour reverse light cycle for at least 1 week prior to experiments. All experiments were conducted in accordance with the NIH Guide for the Care and Use of Laboratory Animals and the Institutional Animal Care and Use Committee at the Medical University of South Carolina.

Chronic intermittent ethanol (CIE) model of alcohol dependence

Ethanol vapor was delivered in Plexiglass inhalation chambers, as previously described[24,25]. Ethanol levels in the chambers were monitored daily and adjusted to maintain blood ethanol levels of 175-250 mg/dL. To confirm target levels were reached, retro-orbital blood was collected from a subset of mice each session. Mice were placed into chambers for 16 hours a day, followed by an 8-hour withdrawal period. Each CIE cycle consisted of 4 days of ethanol exposure in the vapor chambers, followed by a 72-hour withdrawal period. Immediately before being placed in chambers, CIE mice were injected with a loading dose of ethanol (1.6 g/kg) and pyrazole (1 mmol/kg in 0.9% sterile saline; IP), an alcohol dehydrogenase inhibitor. Air control mice were handled in the same manner as CIE mice but placed into chambers with regular room air and were injected with pyrazole (1 mmol/kg in 0.9% sterile saline; IP) immediately before being placed in chambers.

Two-bottle choice preference test

Mice underwent 2-hour two-bottle choice drinking sessions five days/week, beginning 3 hours into the dark cycle in their home cages. One bottle contained 15% (v/v) alcohol, the other contained H_2O or 3% (w/v) sucrose only during alcohol-biased choice test. The side of the alcohol-containing bottle was switched daily to control for habitual responses and side preference. Bottles were weighed before and after drinking sessions to determine the amount consumed, which was normalized to body weight. Preference for alcohol over sucrose was calculated as the percentage of total fluid consumed.

cFos immunohistochemistry

Images of cFos staining in the MD were acquired from brain sections that were originally processed in a published study[26]. In brief, mice underwent 5 alternating weeks of two-bottle choice (15% alcohol vs. H_2O) homecage drinking (or no drinking) and CIE cycles (or Air control). Mice were perfused 2 hours after withdrawal time points of interest: 0, 8, 24, 72 hours, or 7 days. Brains were sliced into 40 µm sections for c-Fos immunohistochemistry. Sections were permeabilized in 0.3% H_2O_2 for 15 minutes, followed by blocking in 2% normal donkey serum in PBS with 0.3% Triton X-100 for 1 hour. Sections were incubated overnight at room temperature in primary antibody diluted in blocking solution (1:20,000 rabbit anti-cFos, EMD-Millipore, catalog # PC38). Sections were then incubated in secondary antibody (1:1000 biotinylated donkey anti-rabbit, Jackson Immuno Research) and ABC (1:1000 Vector Elite Kit, Vector Labs) for 45 minutes. cFos immunostaining was visualized by incubating sections in 0.025% 3,3'-diaminobenzidine (DAB), 0.05% nickel ammonium sulfate, and

0.015% H_2O_2. Images were captured at 4× magnification using an EVOS microscope. Two 40 µm brain sections (approximately -1.34 and -1.70 Bregma) were taken for each animal. Two representative images capturing both the right and left hemispheres were acquired, and cFos-positive nuclei were counted on images using custom settings in ImageJ (adding a bandpass filter and setting noise tolerance at 39). Briefly, a region of interest (ROI) was created using a mouse atlas and was applied to each image to standardize image analysis across slices, and cFos+ cells were identified and counted using ImageJ. cFos counts were normalized to the Air control group for each time point.

Whole-cell slice electrophysiology

Brain slices containing the MD were prepared for whole-cell patch-clamp electrophysiology. Mice were briefly anesthetized with isoflurane before rapidly removing the brain. Brain slices (300 µm) containing the MD were collected using a Leica VT1000S vibratome containing cold oxygenated (95% O2, 5% CO2) sucrose cutting solution (200 mM sucrose, 1.9 mM KCl, 1.2 mM NaH_2PO_4, 6 mM $MgCl_2$, 0.5 mM $CaCl_2$, 0.4 mM ascorbate, 10 mM glucose, and 25 mM $NaHCO_3$, adjusted to 305-315 mOsm, pH 7.4). Slices were transferred into a holding chamber containing oxygenated artificial cerebrospinal fluid (aCSF; 125 mM NaCl, 2.5 mM KCl, 1.25 mM NaH_2PO_4, 1.3 mM $MgCl_2$, 2.0 mM $CaCl_2$, 0.4 mM ascorbate, 10 mM glucose, and 25 mM $NaHCO_3$, adjusted to 290–310 mOsm, pH 7.4) at 34°C for 30 minutes. Slices were kept at room temperature for at least 30 minutes before recording. For recordings, a slice was placed in the recording chambered and perfused with 34°C aCSF at a flow rate of 2 mL/min. Pipettes were prepared from thin-wall borosilicate glass electrodes and were pulled on a Sutter Instrument P97 Micropipette puller with tip resistances from 1.9 to 5.5 MΩ. Current-clamp recordings were conducted in MD principle neurons located using Axon MultiClamp 700B amplifiers (Molecular Devices) and Instrutech ITC-18 analog-digital converters (HEKA instruments) controlled by AxographX software. The patch pipette was filled with potassium gluconate internal solution (120 mM KGluconate, 10 mM KCl, 10 mM HEPES, 2 mM MgCl2, 1 mM EGTA, 2 mM NaATP, and 0.3 mM NaGTP, adjusted to 294 mOsm, pH 7.4). Firing was induced by applying a series of depolarizing and hyperpolarizing current steps (+/- 50, 70, 90, 110 pA) through the patch pipette. Events were filtered at 4 kHz and digitized at a sampling rate of 10 kHz. Recordings were made 2 to 7 hours after euthanasia.

Gene expression analysis

MD tissue samples were collected at 8, 24, 72 hours of withdrawal from 4 weekly cycles of CIE exposure. Adult male mice (n = 7-8/group/time point) were deeply anesthetized via isoflurane and whole brains were rapidly removed. One mm sections containing midline thalamus nuclei were obtained using a stainless-steel mouse brain matrix at 4°C, and the MD was collected from brain sections using a 1 mm tissue punch and immediately flash frozen. Total RNA from MD samples was purified using the ReliaPrep Kit (Promega, Cat # Z6210) following manufacturer's instructions. Direct quantification of transcripts was performed using 100 ng of total RNA on a NanoString nCounter MAX system (NanoString, Seattle, WA) using Mm NeuroPath V1.0 codeset probes. RCC files were imported into nSolver 4.0 software and analyzed using the default criteria. Normalization was performed in nSolver using the geNorm algorithm with 9 housekeeping genes (*Ccdc127*, *Aars*, *Lars*, *Fam104a*, *Mto1*, *Csnk2a2*, *Supt7l*, *Tada2b*, and *Cnot10*) to eliminate sample-to-sample variability. Differentially expressed genes (DEGs) were determined by linear regression analysis in nSolver software, and p-values were corrected using a 5% FDR with the Benjamini, Krieger, and Yekutieli approach in GraphPad Software (version 10.3.0). Functional annotation of the DEGs was performed in ToppGene[27] following our previously published methods[28,29]. To identify potential genes that are regulated by circadian rhythms, genes that differed across time in control mice were queried using the Circadian Genes in Eukaryotes database[30].

In vivo fiber photometry

To induce expression of the calcium sensor GCaMP6f (pENN.AAV1.CamKII.GCaMP6f.WPRE.SV40; Addgene cat# 100834) was unilaterally injected in MD (200 µL; 50 µL/min; AP: -1.58, ML: ±0.44, DV: -3.2). A 2.5 mm fiber optic ferrule containing a 400 µm optical fiber (0.48 NA) was chronically implanted above the injection site (AP: -1.58, ML: ±0.44, DV: -3.1). Mice were allowed to recover for at least 3 weeks prior to the start of experiments. During recording, GCaMP6f was excited using a collimated 470 nm LED (Thorlabs), and signal from an equally powered 405 nm LED was used for normalization to control for movement artifacts. Illumination power for each

LED (5-30 μW) was sinusoidally modulated at 531 Hz (405 nm) and 211 Hz (470 nm) and was passed through Doric fluorescent Mini Cubes. Emission light was focused onto a femtowatt photoreceiver (Newport, model 1672151; DC low setting) and sampled at 6.1 kHz by a RZ5P lock-in digital processor controlled by photometry processing software (Synapse, Tucker-Davis Technologies, Alachua, FL, USA). The GCaMP6f signal was integrated in real-time with licking behavior using lickometer circuits (Med Associates Inc., Fairfax, VT, USA) following our previous methods[31] via TTL inputs to the RZ5P digital processor.

Data were pre-processed using custom written functions in MATLAB (Mathworks) software as described previously[31]. Because the 405 nm and 470 nm signals showed differences in photobleaching over time[31], the signals for each channel were first fitted to a polynomial versus time and then subtracted from one another to calculate the $\Delta F/F$ time series. For detection and quantitation of GCaMP6f events, the 'findpeaks' function in MATLAB was used with values for minimum peak prominence, minimum and maximum peak widths, and minimum peak distance selected by iterative analysis of the data. Transients above a threshold of 2X the median average deviation of the normalized signal were included in the analysis. To analyze calcium signals during drinking sessions, lickometer TTL pulses generated by MedAssociates software were used to define bout start times and duration as described previously[31]. Licking behavior was identified as a bout if lick frequency was >4.5 Hz, interlick interval was <500 ms, and duration was >500 ms based on the known microstructure of rodent drinking behavior[32-34].

Statistical analyses

Data presented represent mean ± SEM and were analyzed with GraphPad Prism (version 10.3.0; GraphPad, La Jolla, CA) or R Statistical software (v4.4.1) using mixed linear models, ANOVAs, or unpaired t-tests. An alpha value of 0.05 was used to determine significance for all analyses. To compare the GCaMP6f signal surrounding drinking bouts, a functional linear mixed model (FLMM)[35] was employed to evaluate calcium signaling associated with alcohol consumption. This model combines linear mixed models with functional regression, enabling a robust analysis of signal intensity variations across multiple covariates, including different solutions (i.e., alcohol vs. water or sucrose), treatment groups, and time points. The signals were aligned at the bout start and the signal during the bout was interpolated (using the median bout duration) so that all data were on the same time scale.

Results

Alcohol dependence and cFos induction in the MD

To first assess how alcohol drinking and dependence affect cellular activity within the MD, we began our investigation by examining the number of cFos+ neurons in the MD using mice exposed to the standard Charleston ARC model of CIE exposure and excessive drinking[24,36-39]. A full description of the methods and the drinking data for this study are described in a recent publication[40] that examined cFos expression across 29 brain regions, which did not include the MD. Regardless of the drinking history, CIE exposure significantly reduced cFos+ cells in the MD at 2 h withdrawal from ethanol vapor chambers in comparison with Air controls (main effect of treatment: $F_{1, 19} = 16.34$, $p = 0.0007$; **Fig 1A,B**). There was a significant increase in cFos+ cells at 10 h of withdrawal in the CIE exposed mice that returned to values below the Air controls at 26 h (main effect of treatment: $F_{1, 20} = 7.117$, $p = 0.0148$). No significant effects of CIE or drinking on cFos expression in the MD were observed at 74 h (main effect of treatment: $F_{1, 20} = 0.6426$, $p = 0.4322$) or 7 d (main effect of treatment: $F_{1, 19} = 1.424$, $p = 0.2475$) withdrawal. Notably, this pattern of cFos expression in the MD was similar to that reported for the lateral OFC, prelimbic cortex, and infralimbic cortex at 2 and 10 h withdrawal[40]. However, the MD was the only region to show reduced number of cFos+ cell density at the 26 h time point (main effect of treatment: $F_{1, 19} = 5.538$, $p = 0.0295$), suggesting that the MD does not merely mimic activity of its cortical connections.

Neuropathology gene expression analysis in alcohol dependent mice

Because excessive drinking can lead to damage of the midline thalamic nuclei[21], we determined how CIE exposure affected signaling pathways and processes using a gene panel that is specific for neuropathology across five cell types: neurons, astrocytes, microglia, oligodendrocytes, and endothelial cells. Due to time differences in tissue collection times, we first examined gene expression differences in air controls to determine

if there were genes regulated by circadian rhythms. There were 15 DEGs in the MD when comparing the 8- vs 24-hour time points, and none when comparing 24- vs 72-hour time points (**Fig 2A**). A search of the Circadian Genes in Eukaryotes database showed that 13 of the 15 DEGs have been linked to circadian rhythms in mice (**Table 1**).

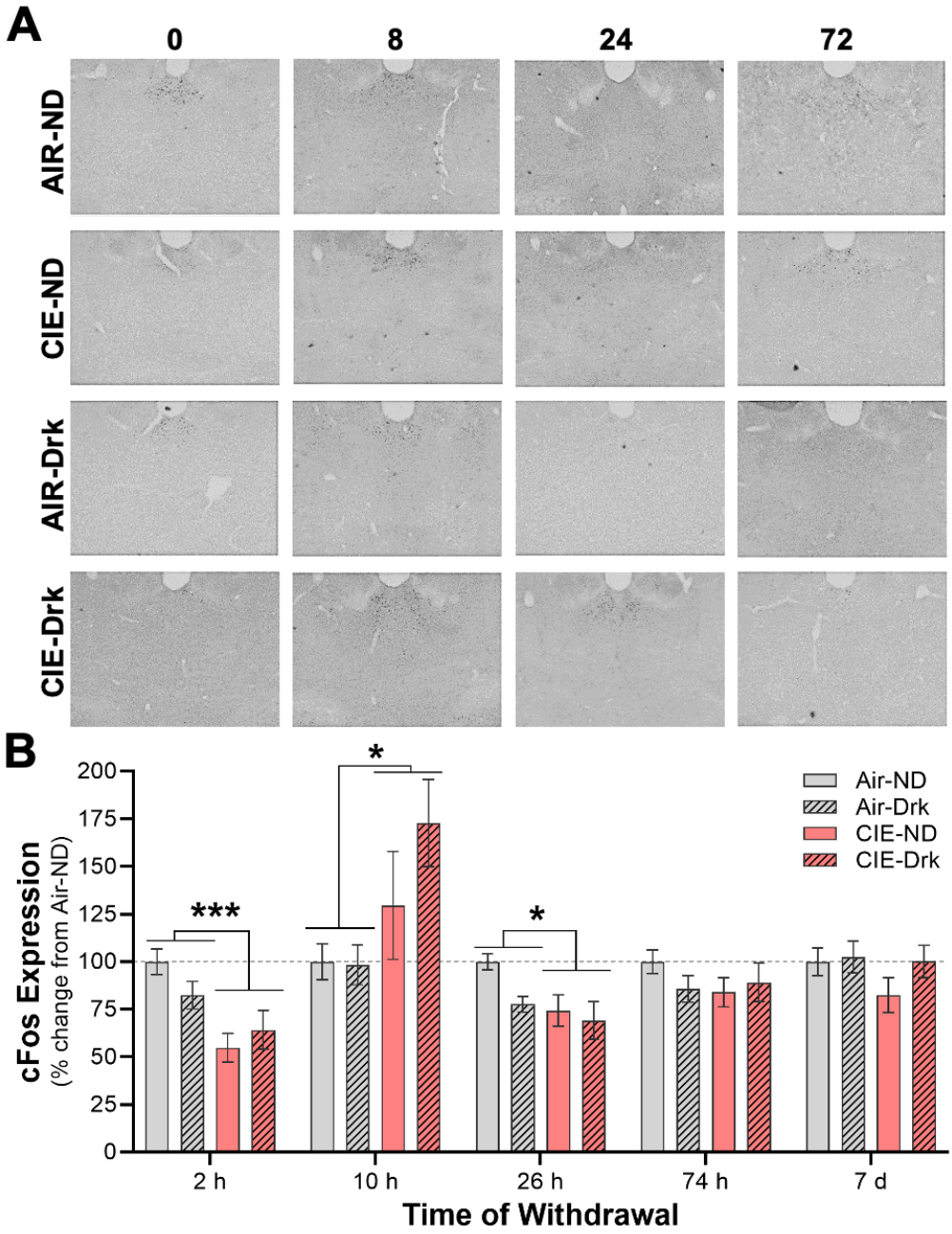

Figure 1 – cFos expression in the MD of non-drinking (ND) and drinking (Drk) C57BL/6J mice that were exposed to air or chronic intermittent ethanol (CIE). (**A**) Representative images and (**B**) analysis of cFos expression in the MD across time and treatment groups (n = 5-6 mice/group/time point; *$p < 0.05$, ***$p<0.001$).

When comparing air controls vs alcohol-exposed mice, differential expression analysis revealed that CIE dysregulated 49 genes in the MD at 8 hours into withdrawal from CIE exposure (**Table 2**; **Fig 2B**), 39 of which were down-regulated. In comparison, CIE exposure did not significantly alter neurodegeneration-related genes at 24 or 72 hours of withdrawal. Gene Ontology enrichment analysis of the DEGs at 8 hours of withdrawal showed that CIE disrupted processes related to glial function, axonal myelination, protein dimerization, and binding for

protein phosphatase, kinase, cytokine receptors, and signaling receptors (**Fig 2C**). The DEGs localized to many different subcellular compartments, including synapses, soma, axons, and membrane rafts.

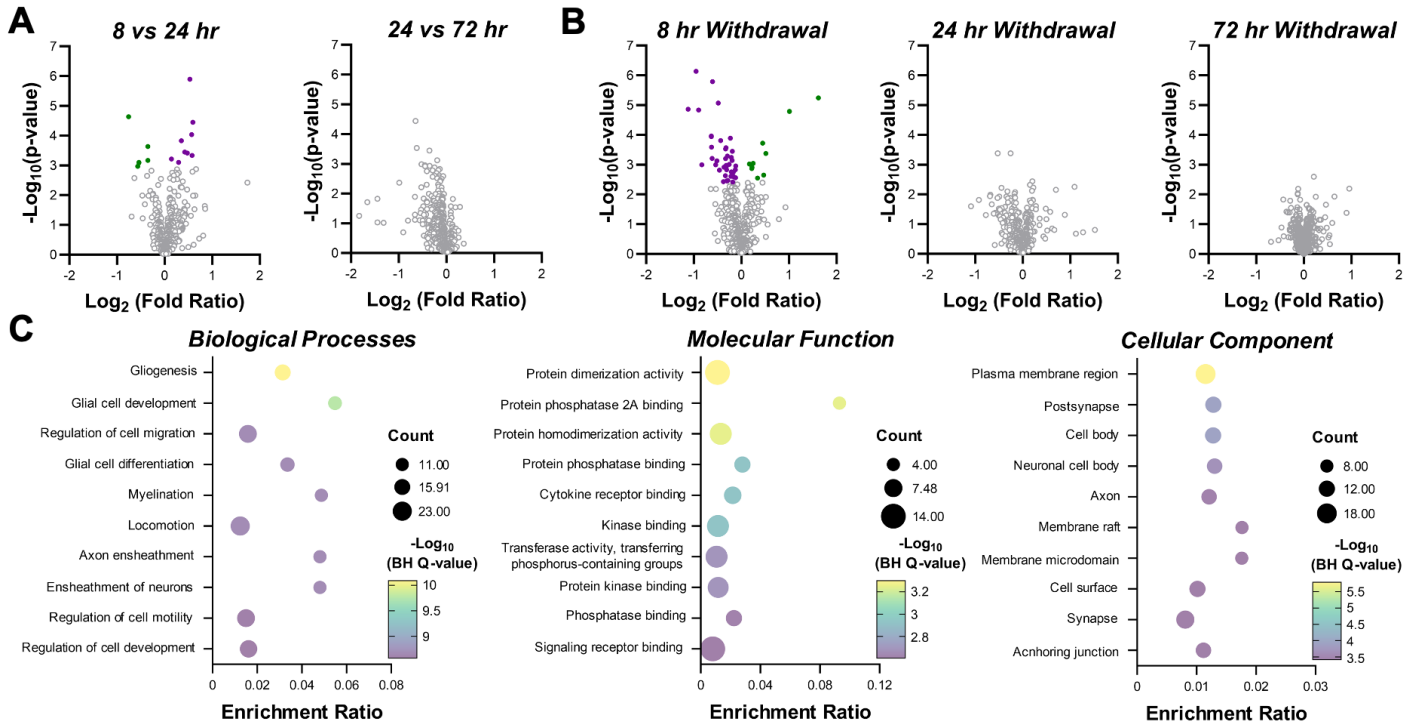

Figure 2 – Differential gene expression analysis in the mediodorsal thalamus of male C57BL/6J mice. Volcano plots comparing gene expression in (**A**) air control mice at different time points of the circadian rhythm and (**B**) air vs CIE exposed mice at 3 time points during withdrawal (n = 7-8 mice/group/time point). (**C**) Gene ontology enrichment analysis of differentially expressed genes in the MD of CIE exposed mice.

Functional adaptations in MD neurons

While we identified MD adaptations during early withdrawal from CIE exposure, it is unclear if there are functional changes at the time point when dependent mice show increased alcohol drinking. Thus, for these studies, we performed slice electrophysiological recordings in MD neurons at 72 hours of withdrawal from CIE exposure. Evoked action potentials were elicited during hyperpolarizing and depolarizing current injections. As shown in **Fig 3A,B**, CIE exposure significantly increased evoked firing of MD neurons in comparison with Air control mice regardless of the polarity of the current injection (main effect of treatment: $F_{1,200} = 43.25$, $p < 0.0001$; n = 7-8 mice/group; 3-6 cells/mouse). Analysis of the biophysical membrane properties of MD neurons revealed a significant decrease in the threshold for action potential firing ($t_{61} = 2.049$, $p < 0.05$; **Fig 3C**) and a trend for a reduction in the medium after-hyperpolarization amplitude ($t_{61} = 1.747$, $p = 0.0857$) in CIE exposed mice. Other measures of MD biophysical membrane properties were not affected by CIE exposure ($p > 0.1$; **Fig 3C**).

Alcohol-biased choice behaviors and MD activity

Alcohol-biased choice behaviors have been described in humans with AUD and in preclinical models of alcohol seeking and dependence[5,7,8,41]. However, little research has focused on how alcohol misuse alters neural activity to modulate this maladaptive behavioral change. To begin to address this, we first replicated alcohol-biased choice using the CIE mouse model of alcohol dependence. Male and female mice were allowed to drink alcohol or water in the two-bottle choice model during a baseline period prior to exposure to air or CIE. Following CIE exposure, mice were given access to sipper tubes containing alcohol and water or sucrose. As expected, CIE exposure increased alcohol intake (**Fig 4A**; main effect of treatment: $F_{1,18} = 4.77$, $p = 0.0425$; n = 5-6 mice/sex/group) and preference (**Fig 4B**; main effect of treatment: $F_{1,18} = 7.86$, $p = 0.0118$) in the alcohol vs

water test drinking sessions. Alcohol drinking was also higher in female compared with male mice (main effect of sex: $F_{1,18} = 4.92$, $p = 0.0397$). When given the choice between alcohol and sucrose, preference for alcohol reduced from >85% to <45% in air controls, whereas preference for alcohol remained relatively high (65-80%) in the CIE exposed mice (**Fig 4C**). Analysis revealed a main effect of treatment ($F_{1,18} = 8.23$, $p = 0.0102$) where preference for alcohol when sucrose was available as an alternative choice was higher in the dependent mice.

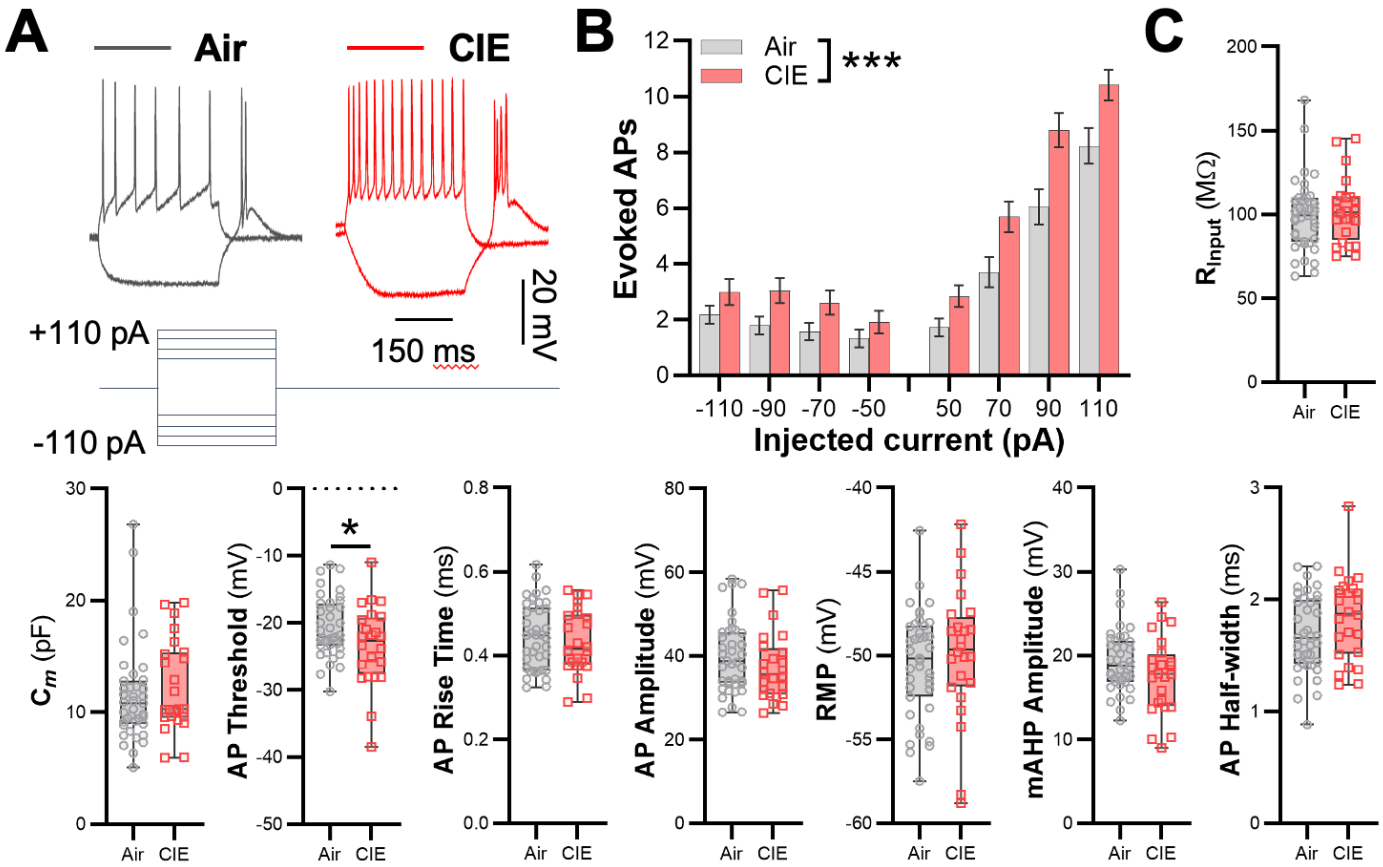

Figure 3 – Evoked action potentials (AP) recorded from neurons in the medial aspect of the MD from control and alcohol dependent male C57BL/6J mice. **A)** Representative traces from hyperpolarizing and depolarizing current steps. **B)** Evoked firing of MD neurons at 72 hours of withdrawal from CIE exposure. **C)** Biophysical membrane properties of MD neurons. (n = 7-8 mice/group; 3-6 cells/mouse; *p < 0.05, ***p < 0.001).

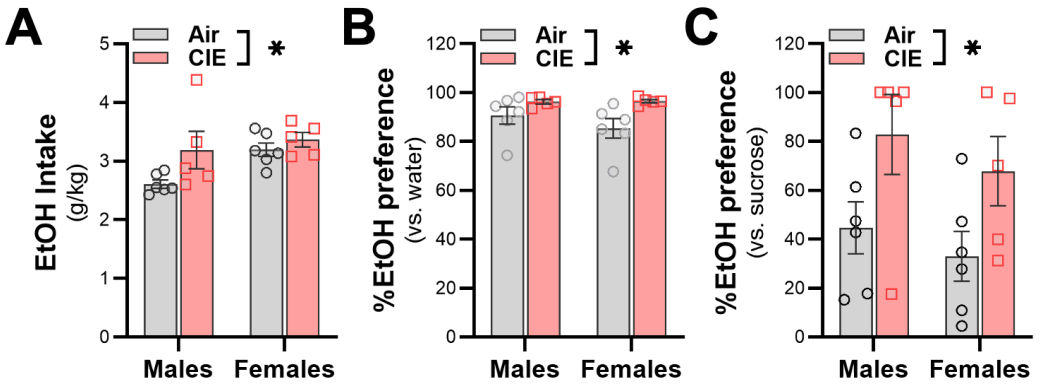

Figure 4 – Drinking in alcohol dependent C57BL/6J mice when given a choice between alcohol and water or sucrose. **A)** Alcohol drinking in CIE exposed male and female mice. Preference for alcohol when given a choice for **B)** water or **C)** sucrose (n = 5-6 mice/group; *p < 0.05).

Elevated MD signaling for alcohol during voluntary drinking

To investigate the impact of chronic alcohol exposure on drinking behavior in relation to MD activity, an AAV encoding for GCaMP6f was infused into the MD and an optical ferrule was implanted (**Fig 5A**) to enable precise collection of calcium signals for fiber photometry. Male C57BL/6J mice (n = 4/group) were given bottles containing 15% alcohol and water across multiple time points: before CIE exposure (Pre-CIE) and after two (Post-CIE 2) or four (Post-CIE 4) cycles of CIE exposure, and drinking behavior was analyzed using a linear mixed model. Ethanol intake increased in CIE-exposed mice compared to air controls (main effect of group: $F_{1,9} = 9.49$, $p = 0.014$; **Fig 5B**). Further, while there was a significant effect of time when comparing ethanol vs. water preference (main effect of time: $F_{2,50} = 4.37$, $p = 0.0178$; **Fig 5C**), post hoc comparisons did not reach significance.

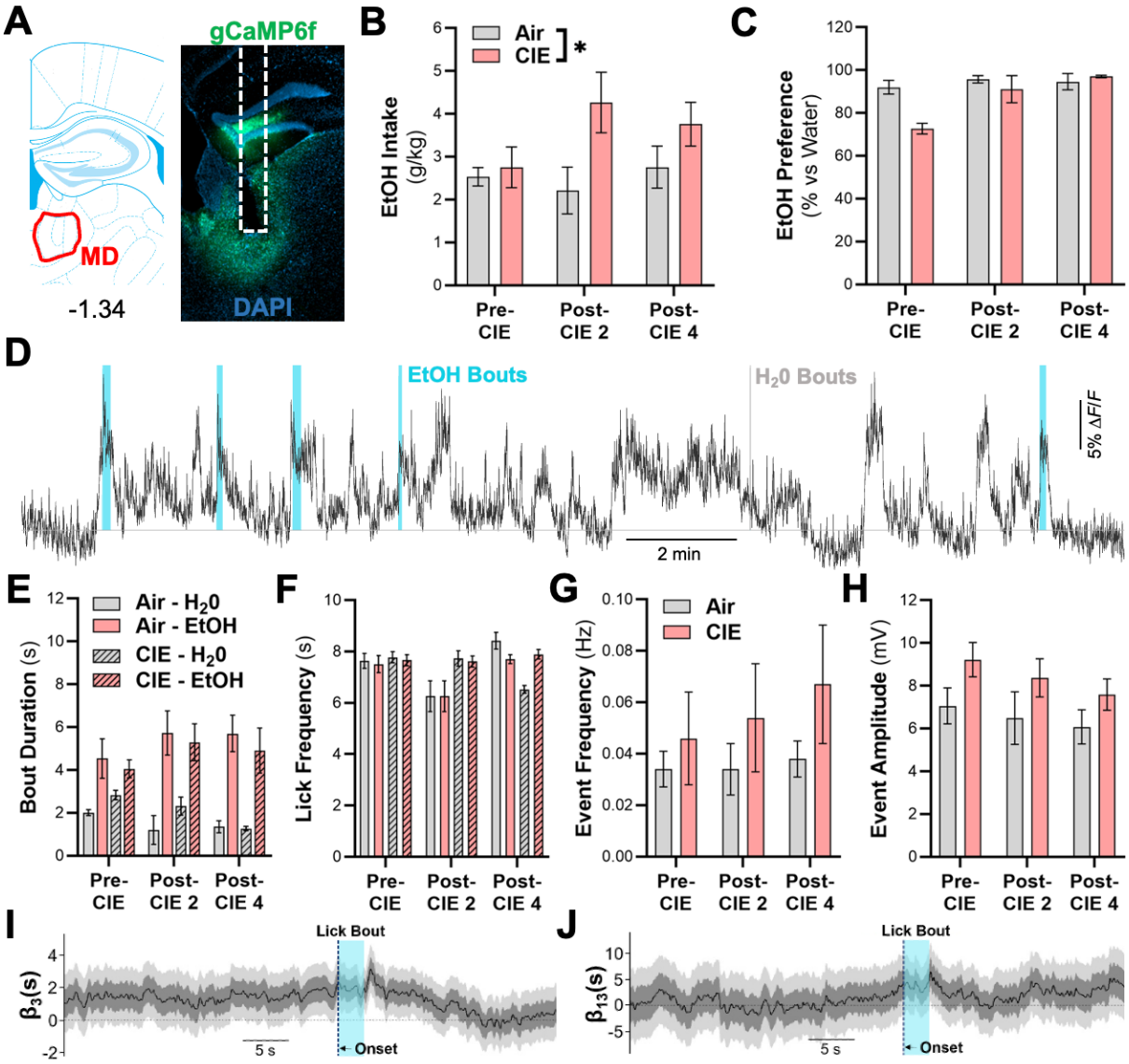

Figure 5 – Alcohol consumption and mediodorsal thalamus (MD) GCaMP6f calcium dynamics in alcohol dependent male C57BL/6J mice. A) Optical ferrule and GCaMP6f expression in the MD for fiber photometry recordings. **B)** Alcohol intake and **C)** preference in CIE-exposed mice versus Air controls across three time points. **D)** Representative GCaMP6f signal in the MD during alcohol and water drinking. Drinking characteristics include **E)** bout duration and **F)** lick frequency during a two-bottle choice test for alcohol and water. Analysis of GCaMP6f **G)** event frequency and **H)** amplitude. FLMM analysis depicting beta coefficients for the calcium signal when comparing **I)** solution (i.e., alcohol vs. water) and **J)** solution-treatment interaction. n = 4 mice/group; *p < 0.05.

A representative fiber photometry recording during an alcohol vs. water drinking session is shown in **Fig 5D**. For these mice, the duration of drinking bouts differed depending on the solution offered with a time-solution interaction (time-solution interaction $F_{2,1087} = 3.43$, $p = 0.0329$), indicating that the influence of the solution on drinking duration changed across different stages of CIE exposure (**Fig 5E**). Specifically, posthoc analyses showed that bout duration for alcohol differed from that for water before CIE exposure ($p < 0.0001$) and after 2 and 4 weeks of CIE exposure ($p = 0.0043$). The duration of alcohol drinking bouts increased throughout CIE exposure, notably when comparing bout duration before CIE exposure to both 2 ($p = 0.0026$) and 4 ($p = 0.0331$) weeks of CIE exposure. Lick frequency varied not only by the type of solution but across different groups and time points (group-time-solution interaction: $F_{1,1089} = 4.69$, $p = 0.0093$; **Fig 5F**). Posthoc tests revealed differences in lick frequency between water and alcohol after 2 weeks of CIE exposure ($p = 0.0482$). Analysis revealed a significant main effect of time for GCaMP6f events ($F_{2,51} = 4.44$, $p = 0.0166$; **Fig 5G**), but posthoc analysis did not show significant differences between CIE cycles. Furthermore, analysis of the amplitude of GCaMP6f events did not reveal significant changes across treatment groups or time (**Fig 5H**). When comparing the calcium signal 30 seconds before, during, and 30 seconds after drinking bouts in each group across time, the beta coefficient, a measure reflecting the relative strength of the calcium response to alcohol, was significantly different during and following drinking bouts (β coefficient plus confidence interval > 0), suggesting elevated calcium activity specific to alcohol (main effect of solution; **Fig 5I**). The interaction between solution and treatment did not reveal differences in the signal surrounding drinking bouts (**Fig 5J**).

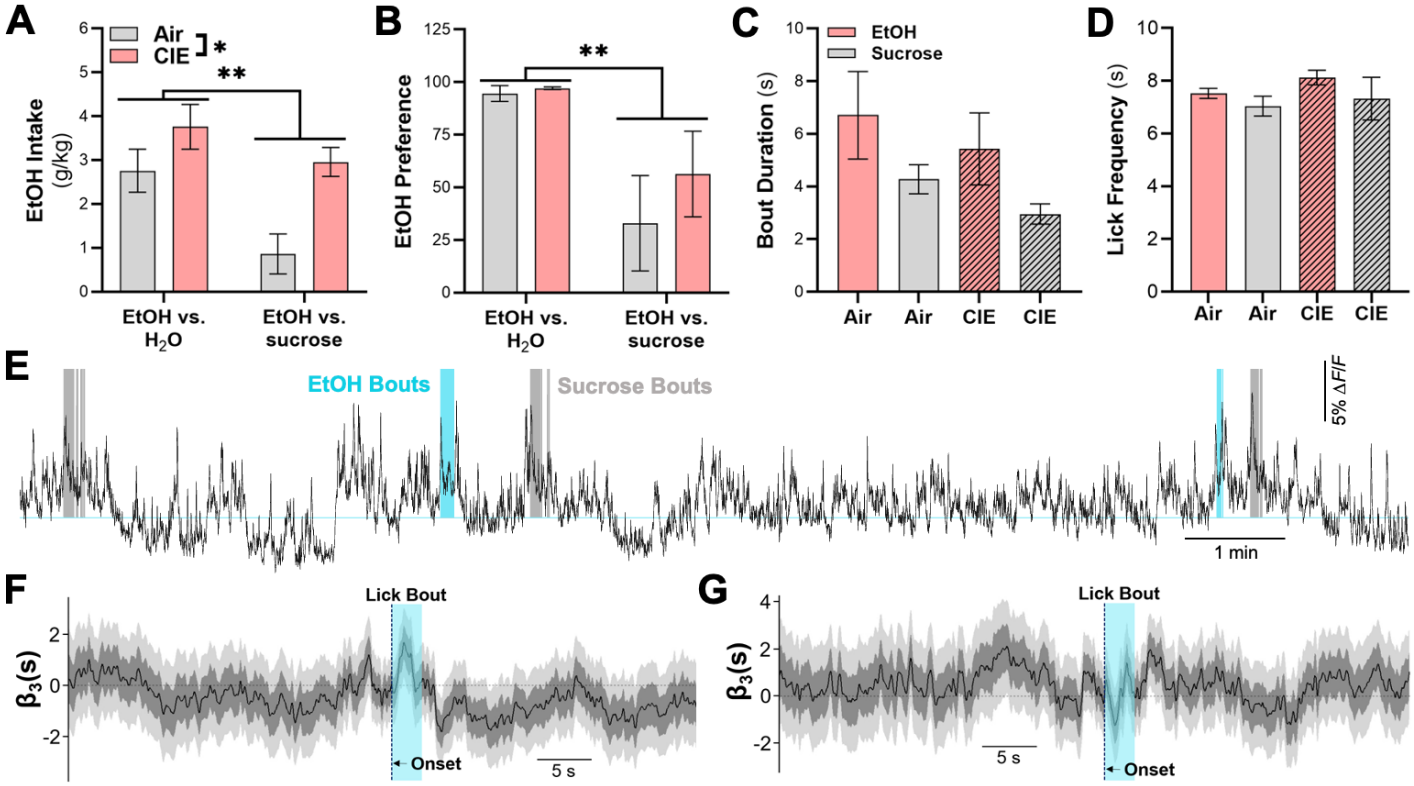

Figure 6 – Drinking behavior and MD activity in alcohol dependent C57BL/6J mice when give a choice between alcohol and sucrose. A) Alcohol intake and **B)** preference in the presence of a choice for alcohol and water or alcohol and 3% sucrose. **C)** Bout duration and **D)** lick frequency during alcohol choice drinking sessions. **E)** Example fiber photometry recording of MD calcium activity during an alcohol and sucrose drinking session. **F)** FLMM analysis of beta coefficients for solution (alcohol vs. sucrose) and **G)** solution by treatment interaction. n = 4 mice/group; *p < 0.05, **p < 0.005.

Next, we interrogated MD signaling during choice behavior for alcohol in the presence of an alternative reward. After completing the alcohol vs. water drinking session post-CIE exposure, mice underwent a two-bottle choice test for alcohol vs. 3% sucrose. In dependent mice, alcohol intake was significantly higher than air controls in the sucrose choice session (main effect of group: $F_{1,6} = 8.38$, $p = 0.026$; main effect of time: $F_{1,10} = 10.49$, $p = 0.009$; **Fig 6A**). Alcohol preference significantly decreased in the alcohol vs sucrose choice session compared to when water was the alternative choice with alcohol (main effect of time: $F_{1,9} = 18.964$, $p = .002$; **Fig 6B**). Analysis of bout duration and lick frequency indicated a significant main effect of solution (bout duration: $F_{2,623} = 7.741$, $p < 0.001$; lick frequency: $F_{2,623} = 5.072$, $p < 0.001$; **Fig 6C,D**), where alcohol was greater than sucrose for both measures. A representative fiber photometry recording during an alcohol vs. sucrose drinking session is shown in **Fig 6E**. When comparing the signal for alcohol and sucrose during choice drinking, the beta coefficient of the calcium signal was briefly but significantly elevated during drinking bouts (**Fig 6F**). The interaction between solution and treatment did not reveal differences in the signal surrounding drinking bouts (**Fig 6G**).

Discussion

Because of its involvement in reward-guided and cognitive behaviors and its interconnections with cortical brain regions, we explored neuroadaptations and in vivo signaling in the MD of alcohol dependent mice. We found time-dependent differences in cellular activation and neuropathology-related gene expression during acute (<24 hours) and protracted (3-7 days) withdrawal from chronic alcohol exposure in male C57BL/6J mice. There were functional changes in membrane excitability of MD neurons at a time point where dependent mice consume more alcohol than control mice. In this study, alcohol dependent male and female mice also showed a strong preference for alcohol over a natural reward when given a choice between the two solutions in a home cage drinking model. Using in vivo fiber photometry during home cage drinking sessions, we observed increased activity of MD neurons surrounding alcohol drinking bouts that was more pronounced on days when water was given as a choice solution compared with sucrose. Overall, this study shows molecular and functional adaptations in the MD using a dependence model that increases alcohol drinking and shifts preference toward alcohol over a naturally rewarding solution.

Functional adaptations in the MD of dependent mice

To map activity changes in the MD across acute and protracted withdrawal from CIE exposure, we first measured cFos expression in control and alcohol dependent mice at five different time points. Similar to its cortical partners, cFos was reduced after removal from vapor chambers while mice were still intoxicated and increased at the peak of withdrawal hyperexcitability. Perhaps due to differences in the severity of alcohol exposure models, early withdrawal from an alcohol liquid diet did not activate cFos in the MD[23] in wildtype mice, but increased cFos in PKC-ε KO mice. This suggests a possible genetic component to MD activation during acute alcohol withdrawal, although *Prkce* expression was not altered in the current study, which contrasts the increased expression that has been reported in other model systems and brain regions[42-45]. When compared to its interconnected cortical regions and 24 other brain regions analyzed in Smith et al.[26] that showed no change or elevated cFos at 1 day of withdrawal, we observed a reduction in cFos expression in the MD, demonstrating a unique response of the MD during withdrawal from CIE exposure in C57BL/6J mice. cFos expression in the MD returned to control values at 3-7 days of withdrawal, which was also unique compared to the reduced expression observed in the prelimbic and infralimbic cortices at these later withdrawal time points[26]. Thus, we showed that the MD is differentially activated across acute and prolonged alcohol withdrawal that does not always parallel the response pattern in its interconnected cortical regions.

Next, we interrogated functional adaptations in MD neuron cell firing at a time point when dependent mice show increased alcohol drinking[24]. While cFos expression did not differ between control and CIE exposed mice at 3 days of withdrawal, excitability was increased in the alcohol dependent mice following both depolarizing and hyperpolarizing current steps. With the exception of the action potential threshold, which was decreased in the dependent mice, CIE exposure did not alter other biophysical membrane properties of MD neurons. Whereas evoked action potentials during depolarizing pulse are driven by Na^+ spikes, the rebound burst firing following hyperpolarization pulses in thalamic neurons are mediated by low-voltage activated T-type Ca^{2+} channels. In

mouse nucleus reuniens, CIE exposure increased low-threshold bursts and T-type Ca^{2+} channel gene expression and shifted T-type Ca^{2+} channel gating properties during acute (<1 d), but not protracted (>1 d) withdrawal[46]. Compared with the reuniens, functional adaptations in rebound burst firing persist for a longer duration during withdrawal in the MD of dependent mice. The mechanisms underlying the increased excitability of Na^{+} and Ca^{2+} spikes in MD neurons from dependent mice are unknown at this point, but may be driven by multiple disrupted processes, including shifts in T-type Ca^{2+} channel expression or gating properties that will be explored in future studies.

Transcriptomic adaptations in dependent mice

Examination of a neuropathology gene panel revealed differential expression of genes in alcohol dependent mice at 8 hours of withdrawal, but not at later time points. Enrichment analysis clustered the DEGs into processes related to glial function, axonal myelination, and protein binding. Our results add to a growing literature that alcohol drinking and dependence induce genetic and morphological changes in microglial[47-54] and astrocytes[55-57]. None of the genes included in the panel as markers of neurons were differentially expressed, and only a few DEGs (*Emcn*, *Icam2*, *Tie1*) are markers of endothelial cells. Also, neither 'apoptosis' nor 'endothelial cell function' were identified as top terms in the enrichment analysis. There is profound neuronal loss in the mediodorsal thalamic nucleus in AUD individuals with Wernicke-Korsakoff syndrome[21], and a recent tractography study using diffusion tensor imaging and high resolution MRI identified degeneration of white matter tracts interconnecting the MD and the PFC in individuals with AUD[13]. It is possible that neuronal degeneration went undetected in our study or the CIE model does not produce widespread neural damage or changes in blood-brain barrier integrity based on evidence using this neuropathology panel. However, we did observe dysregulation of cell firing that might reflect changes in genes that control axonal processes and myelination. It is also possible that CIE exposure produces unique genetic adaptations in specific circuits (e.g., MD→PFC) that went undetected using our bulk tissue approach. Thus, while these studies identified adaptations in transcripts for specific biological processes, further studies are necessary to examine the full extent of genetic and cell-type specific changes that occur across time in the MD of dependent mice.

In addition to the DEGs identified in CIE exposed mice, we also identified DEGs when comparing different time points in the circadian rhythm of alcohol-naïve mice. A searching the Circadian Genes in Eukaryotes database confirmed that the majority (13 of 15) have been linked to circadian rhythms in mice, partially validating results from the gene panel analysis. Many of the genes were identified as having a role in circadian rhythms based on studies in the liver and superchiasmatic nucleus, an organ and brain region with known pacemaker actions for controlling metabolic and physiological processes. Evidence suggests that the MD is involved in processes related to several aspects of circadian rhythms, including arousal[58], sleep[20,59,60], and time perception[61], although the exact role of the MD DEGs in controlling physiological processes important for circadian rhythms is unknown. Interestingly, expression of two of the circadian-related DEGs (*Egr1* and *Gtf2ird1*) were also differentially expressed in the MD of CIE exposed mice. Individuals with AUD often shown signs of circadian misalignment, including disrupted sleep cycles, body temperature, and altered molecular rhythms and neuroendocrinological functions[62-66]. Our findings suggest that these DEGs in the MD could control some aspects of circadian rhythms, and that the transcription factors *Egr1* and *Gtf2ird1* are potential candidate genes for perturbation of circadian alignment in AUD.

Alcohol-biased choice and MD activity

In a home cage choice model for alcohol or a non-drug reward, we showed that preference for alcohol remained high in male and female C57BL/6J mice exposed to CIE. In both sexes, alcohol intake and preference increased in the dependent mice and preference for alcohol over water in both groups and sexes was > 80%. However, when given a choice between alcohol and sucrose in their home cage, preference for alcohol in the control mice dropped to below 45%, demonstrating that the CIE dependence model establishes a phenotype where a high preference for alcohol over a non-drug reward is maintained. While previous preclinical studies showed preference for alcohol over saccharin and social reward in operant models in rats, we extended these findings to a voluntary choice home cage drinking model in C57BL/6J mice. Consistent with the preference choice for alcohol over social rewards in male and female rats[6,7], we showed that induction of alcohol dependence maintains preference for alcohol over sucrose in both sexes providing another model to assess alcohol-biased

choice behaviors that have been described in AUD[41]. Using fiber photometry recordings of the MD during home cage drinking, we showed MD activity increases around bouts for alcohol, water, and sucrose. In the MD, signaling before and during alcohol licking bouts was significant higher than bouts for water, and the difference in MD signaling for alcohol over water was maintained in alcohol dependent mice. In control and dependent mice given a choice between alcohol and sucrose, there was a modest but significant increase in the MD signal for alcohol during drinking bouts. Thus, in a model that maintains high preference for alcohol over water and a non-drug reward, these studies demonstrated unique signaling in the MD during alcohol consumption.

In summary, these studies demonstrate functional and transcriptomic adaptations in the MD of alcohol dependent mice in a model that produces excessive drinking and biased choice behaviors for alcohol over a natural reward. We also showed a unique signature of MD activity for alcohol drinking that was maintained in dependent mice. Further work is necessary to determine the role of the MD in controlling alcohol-biased choice behaviors and if the differentially expressed genes identified in this study regulate circadian processes and alcohol-related behaviors, such as drinking, sleep disturbances, or preference for alcohol over natural rewards.

Acknowledgments

Supported in part by the Charleston Alcohol Research Center (P50 AA010761), the Cellular, Biochemical and Molecular Sciences Training Program (T32 GM132055), the Summer Undergraduate Research Program in Neuroscience of Addiction (R25 DA033680), Training in Alcohol Research Program (T32 AA007474), the Translational Science Laboratory Core, Hollings Cancer Center Shared Resources, Medical University of South Carolina (P30 CA138313), and NIH grants K01 AA025110 (JAR) and R01 AA023288 (PJM).

Table 1. Differentially expressed genes in the mediodorsal thalamus of control male C57BL/6J mice and their relation to circadian rhythms. SCN, Suprachiasmatic nucleus.

Gene	Log_2 Fold Change	p-Value	q-Value	PMID for Circadian Rhythms	Tissue
Tnfrsf12a	-0.758	2.32^{-05}	0.00775	26523393	SCN
Xbp1	-0.566	0.00107	0.04764	26523393	SCN
Bdnf	-0.54	0.00078	0.03897	23217262	Liver
Cldn5	-0.539	0.00082	0.03897	17550994; 26341910; 26523393; 16230482	SCN; Skeletal muscle; Hippocampus; Aorta
Gss	-0.352	0.00023	0.02582	19343201; 22629359; 24360271	Liver
Gtf2ird1	-0.352	0.00069	0.03897	23896777; 19343201; 24591654; 26523393; 24360271	SCN; Cartilage; Liver
Hif1a	0.143	0.00061	0.03897	26523393	SCN
Mag	0.293	0.00079	0.03897	26523393; 23217262	SCN; Liver
Tcerg1	0.352	0.00015	0.01977	26523393	SCN
Mog	0.423	0.00036	0.03205	n/a	n/a
Trem2	0.479	0.00038	0.03205	n/a	n/a
Fus	0.532	1.26^{-06}	0.00084	16998155; 26341910; 24360271; 22753467; 22629359; 22440902; 19343201	Hippocampus; Adrenal gland; Liver; Kidney; Epidermis
Egr1	0.569	9.16^{-05}	0.01529	24672008; 26393668; 26471974; 22629359; 26486724; 29138967	Retina; Liver; SCN
Pllp	0.576	0.00046	0.03406	17550994; 24360271	Skeletal muscle; Liver
Bid	0.594	3.54^{-05}	0.00788	19343201	Liver

Table 2. Differentially expressed genes in the mediodorsal thalamus of CIE exposed male C57BL/6J mice.

Gene	Log_2 fold change	p-value	q-value
Icam2	-1.12	1.39^{-05}	0.00148
Mmp14	-0.951	7.18^{-07}	0.00046
Hspb1	-0.899	1.46^{-05}	0.00148
Nes	-0.832	0.00010	0.02269
Ugt8a	-0.633	0.00012	0.00824
Eng	-0.63	0.00011	0.00824
P2ry12	-0.626	0.00026	0.01216
Aqp4	-0.613	0.00061	0.01943
Car2	-0.606	1.63^{-06}	0.00052
Adra2a	-0.538	0.00010	0.02269
Erbb3	-0.515	0.00074	0.02046
Adcy8	-0.487	8.57^{-06}	0.00137
Tie1	-0.459	0.00150	0.02592
Cxcl12	-0.437	0.00015	0.00895
Lpar1	-0.379	0.00370	0.04920
Emcn	-0.366	0.00120	0.02364
Gtf2ird1	-0.337	0.00240	0.03681
Plxnb3	-0.331	0.00030	0.01262
Bcl2	-0.33	0.00064	0.01943
Notch1	-0.321	0.00027	0.01211
Akt2	-0.32	0.00104	0.02269
AI464131	-0.311	0.00147	0.02592
Gjb1	-0.309	0.00109	0.02269
Cx3cr1	-0.307	0.00348	0.04735
Fa2h	-0.292	0.00052	0.01830
Olig2	-0.286	0.00340	0.04726
Csf1r	-0.255	0.00098	0.02269
Bcas1	-0.233	0.00013	0.00831
Spast	-0.219	0.00246	0.03745
Adam10	-0.211	0.00058	0.01943
Parp1	-0.211	0.00174	0.02886
Pla2g16	-0.195	0.00072	0.02046
Gnai1	-0.191	0.00035	0.01415
Mapt	-0.18	0.00377	0.04920
Efna5	-0.17	0.00176	0.02886
Pgk1	-0.158	0.00255	0.03792
Akt1	-0.129	0.00148	0.02592
Myh10	-0.124	0.00278	0.04007
Nf1	-0.118	0.00110	0.02269
Pik3r1	0.168	0.00095	0.02269
Ache	0.217	0.00136	0.02558
Twistnb	0.224	0.00122	0.02364
Mal	0.248	0.00090	0.02269
Sirt7	0.341	0.00282	0.04007
Slc2a1	0.448	0.00019	0.01007
Angpt2	0.469	0.00225	0.03597
Egr1	0.515	0.00042	0.01572
Ddc	1.01	1.62^{-05}	0.00148
Cdkn1a	1.62	5.72^{-06}	0.00122

References

1 Manthey, J. *et al.* Global alcohol exposure between 1990 and 2017 and forecasts until 2030: a modelling study. *Lancet* **393**, 2493-2502, doi:10.1016/S0140-6736(18)32744-2 (2019).

2 Ariesen, A. D., Neubert, J. H., Gaastra, G. F., Tucha, O. & Koerts, J. Risky Decision-Making in Adults with Alcohol Use Disorder-A Systematic and Meta-Analytic Review. *J Clin Med* **12**, doi:10.3390/jcm12082943 (2023).

3 Wicker, E., Turchi, J., Malkova, L. & Forcelli, P. A. Mediodorsal thalamus is required for discrete phases of goal-directed behavior in macaques. *Elife* **7**, doi:10.7554/eLife.37325 (2018).

4 Wiers, C. E. *et al.* Comparing Three Cognitive Biases for Alcohol Cues in Alcohol Dependence. *Alcohol Alcohol* **52**, 242-248, doi:10.1093/alcalc/agw063 (2017).

5 Augier, E. *et al.* A molecular mechanism for choosing alcohol over an alternative reward. *Science* **360**, 1321-1326, doi:10.1126/science.aao1157 (2018).

6 Augier, G. *et al.* Wistar rats choose alcohol over social interaction in a discrete-choice model. *Neuropsychopharmacology* **48**, 1098-1107, doi:10.1038/s41386-022-01526-8 (2023).

7 Marchant, N. J. *et al.* Rats choose alcohol over social reward in an operant choice procedure. *Neuropsychopharmacology* **48**, 585-593, doi:10.1038/s41386-022-01447-6 (2023).

8 Russo, M., Funk, D., Loughlin, A., Coen, K. & Le, A. D. Effects of alcohol dependence on discrete choice between alcohol and saccharin. *Neuropsychopharmacology* **43**, 1859-1866, doi:10.1038/s41386-018-0101-1 (2018).

9 Parnaudeau, S., Bolkan, S. S. & Kellendonk, C. The Mediodorsal Thalamus: An Essential Partner of the Prefrontal Cortex for Cognition. *Biol Psychiatry* **83**, 648-656, doi:10.1016/j.biopsych.2017.11.008 (2018).

10 Savage, L. M., Nunes, P. T., Gursky, Z. H., Milbocker, K. A. & Klintsova, A. Y. Midline Thalamic Damage Associated with Alcohol-Use Disorders: Disruption of Distinct Thalamocortical Pathways and Function. *Neuropsychol Rev* **31**, 447-471, doi:10.1007/s11065-020-09450-8 (2021).

11 Bolkan, S. S. *et al.* Thalamic projections sustain prefrontal activity during working memory maintenance. *Nat Neurosci* **20**, 987-996, doi:10.1038/nn.4568 (2017).

12 Lyuboslavsky, P., Ordemann, G. J., Kizimenko, A. & Brumback, A. C. Two contrasting mediodorsal thalamic circuits target the mouse medial prefrontal cortex. *J Neurophysiol* **131**, 876-890, doi:10.1152/jn.00456.2023 (2024).

13 Segobin, S. *et al.* Dissociating thalamic alterations in alcohol use disorder defines specificity of Korsakoff's syndrome. *Brain* **142**, 1458-1470, doi:10.1093/brain/awz056 (2019).

14 Vertes, R. P. Analysis of projections from the medial prefrontal cortex to the thalamus in the rat, with emphasis on nucleus reuniens. *J Comp Neurol* **442**, 163-187, doi:10.1002/cne.10083 (2002).

15 Chakraborty, S., Kolling, N., Walton, M. E. & Mitchell, A. S. Critical role for the mediodorsal thalamus in permitting rapid reward-guided updating in stochastic reward environments. *Elife* **5**, doi:10.7554/eLife.13588 (2016).

16 Alcaraz, F. *et al.* Thalamocortical and corticothalamic pathways differentially contribute to goal-directed behaviors in the rat. *Elife* **7**, doi:10.7554/eLife.32517 (2018).

17 Fredericksen, K. E., McQueen, K. A. & Samuelsen, C. L. Experience-Dependent c-Fos Expression in the Mediodorsal Thalamus Varies With Chemosensory Modality. *Chem Senses* **44**, 41-49, doi:10.1093/chemse/bjy070 (2019).

18 Courtiol, E. & Wilson, D. A. Neural Representation of Odor-Guided Behavior in the Rat Olfactory Thalamus. *J Neurosci* **36**, 5946-5960, doi:10.1523/JNEUROSCI.0533-16.2016 (2016).

19 Salling, M. C. *et al.* Cue-induced reinstatement of alcohol-seeking behavior is associated with increased CaMKII T286 phosphorylation in the reward pathway of mice. *Pharmacol Biochem Behav* **163**, 20-29, doi:10.1016/j.pbb.2017.10.011 (2017).

20 Choi, S., Yu, E., Lee, S. & Llinas, R. R. Altered thalamocortical rhythmicity and connectivity in mice lacking CaV3.1 T-type Ca2+ channels in unconsciousness. *Proc Natl Acad Sci U S A* **112**, 7839-7844, doi:10.1073/pnas.1420983112 (2015).

21 Halliday, G., Cullen, K. & Harding, A. Neuropathological correlates of memory dysfunction in the Wernicke-Korsakoff syndrome. *Alcohol Alcohol Suppl* **2**, 245-251 (1994).

22 Shibasaki, M., Inoue, M., Kurokawa, K., Ogou, S. & Ohkuma, S. Expression of serotonin transporter in mice with ethanol physical dependency. *J Pharmacol Sci* **114**, 234-237, doi:10.1254/jphs.10146sc (2010).
23 Olive, M. F. *et al.* Reduced ethanol withdrawal severity and altered withdrawal-induced c-fos expression in various brain regions of mice lacking protein kinase C-epsilon. *Neuroscience* **103**, 171-179, doi:10.1016/s0306-4522(00)00566-2 (2001).
24 Padula, A. E. *et al.* KCNN Genes that Encode Small-Conductance Ca2+-Activated K+ Channels Influence Alcohol and Drug Addiction. *Neuropsychopharmacology* **40**, 1928-1939, doi:10.1038/npp.2015.42 (2015).
25 Padula, A. E. *et al.* Bioinformatics identification and pharmacological validation of Kcnn3/K(Ca)2 channels as a mediator of negative affective behaviors and excessive alcohol drinking in mice. *Transl Psychiatry* **10**, 414, doi:10.1038/s41398-020-01099-4 (2020).
26 Smith, R. J. *et al.* Dynamic c-Fos changes in mouse brain during acute and protracted withdrawal from chronic intermittent ethanol exposure and relapse drinking. *Addict Biol* **25**, e12804, doi:10.1111/adb.12804 (2020).
27 Chen, J., Bardes, E. E., Aronow, B. J. & Jegga, A. G. ToppGene Suite for gene list enrichment analysis and candidate gene prioritization. *Nucleic Acids Res* **37**, W305-311, doi:10.1093/nar/gkp427 (2009).
28 Womersley, J. S. *et al.* Adaptations in glutathione-based redox protein signaling pathways and alcohol drinking across species. *Biomed Pharmacother* **180**, 117514, doi:10.1016/j.biopha.2024.117514 (2024).
29 Mulholland, P. J. *et al.* Adaptor protein complex 2 in the orbitofrontal cortex predicts alcohol use disorder. *Mol Psychiatry* **28**, 4766-4776, doi:10.1038/s41380-023-02236-3 (2023).
30 Li, S. *et al.* CGDB: a database of circadian genes in eukaryotes. *Nucleic Acids Res* **45**, D397-D403, doi:10.1093/nar/gkw1028 (2017).
31 Rinker, J. A. *et al.* Prelimbic neuron calcium activity predicts perceived hedonic value across drinking solutions and ethanol dependent states in mice. *bioRxiv*, 2023.2004.2004.535635, doi:10.1101/2023.04.04.535635 (2023).
32 Johnson, A. W. *et al.* An analysis of licking microstructure in three strains of mice. *Appetite* **54**, 320-330, doi:10.1016/j.appet.2009.12.007 (2010).
33 Davis, J. D. & Smith, G. P. Analysis of the microstructure of the rhythmic tongue movements of rats ingesting maltose and sucrose solutions. *Behav Neurosci* **106**, 217-228 (1992).
34 Boughter, J. D., Jr., Baird, J. P., Bryant, J., St John, S. J. & Heck, D. C57BL/6J and DBA/2J mice vary in lick rate and ingestive microstructure. *Genes Brain Behav* **6**, 619-627, doi:10.1111/j.1601-183X.2006.00293.x (2007).
35 Loewinger, G., Cui, E., Lovinger, D. M. & Pereira, F. A Statistical Framework for Analysis of Trial-Level Temporal Dynamics in Fiber Photometry Experiments. *bioRxiv*, doi:10.1101/2023.11.06.565896 (2024).
36 Griffin, W. C., 3rd, Lopez, M. F., Yanke, A. B., Middaugh, L. D. & Becker, H. C. Repeated cycles of chronic intermittent ethanol exposure in mice increases voluntary ethanol drinking and ethanol concentrations in the nucleus accumbens. *Psychopharmacology (Berl)* **201**, 569-580, doi:10.1007/s00213-008-1324-3 (2009).
37 Griffin, W. C., 3rd, Lopez, M. F. & Becker, H. C. Intensity and duration of chronic ethanol exposure is critical for subsequent escalation of voluntary ethanol drinking in mice. *Alcohol Clin Exp Res* **33**, 1893-1900, doi:10.1111/j.1530-0277.2009.01027.x (2009).
38 Lopez, M. F. & Becker, H. C. Effect of pattern and number of chronic ethanol exposures on subsequent voluntary ethanol intake in C57BL/6J mice. *Psychopharmacology (Berl)* **181**, 688-696, doi:10.1007/s00213-005-0026-3 (2005).
39 Becker, H. C. & Lopez, M. F. Increased ethanol drinking after repeated chronic ethanol exposure and withdrawal experience in C57BL/6 mice. *Alcohol Clin Exp Res* **28**, 1829-1838, doi:10.1097/01.alc.0000149977.95306.3a (2004).
40 Smith, R. J. *et al.* Dynamic c-Fos changes in mouse brain during acute and protracted withdrawal from chronic intermittent ethanol exposure and relapse drinking. *Addict Biol*, e12804, doi:10.1111/adb.12804 (2019).
41 Hogarth, L. & Field, M. Relative expected value of drugs versus competing rewards underpins vulnerability to and recovery from addiction. *Behav Brain Res* **394**, 112815, doi:10.1016/j.bbr.2020.112815 (2020).

42 Messing, R. O., Petersen, P. J. & Henrich, C. J. Chronic ethanol exposure increases levels of protein kinase C delta and epsilon and protein kinase C-mediated phosphorylation in cultured neural cells. *J Biol Chem* **266**, 23428-23432 (1991).
43 Kumar, J., Hapidin, H., Get Bee, Y. T. & Ismail, Z. The effects of acute ethanol administration on ethanol withdrawal-induced anxiety-like syndrome in rats: A biochemical study. *Alcohol* **50**, 9-17, doi:10.1016/j.alcohol.2015.10.001 (2016).
44 Hanim, A. *et al.* Alcohol Dependence Modulates Amygdalar mTORC2 and PKCepsilon Expression in a Rodent Model. *Nutrients* **15**, doi:10.3390/nu15133036 (2023).
45 McClintick, J. N. *et al.* Ethanol treatment of lymphoblastoid cell lines from alcoholics and non-alcoholics causes many subtle changes in gene expression. *Alcohol* **48**, 603-610, doi:10.1016/j.alcohol.2014.07.004 (2014).
46 Graef, J. D., Huitt, T. W., Nordskog, B. K., Hammarback, J. H. & Godwin, D. W. Disrupted thalamic T-type Ca2+ channel expression and function during ethanol exposure and withdrawal. *J Neurophysiol* **105**, 528-540, doi:10.1152/jn.00424.2010 (2011).
47 Melbourne, J. K., Wooden, J. I., Carlson, E. R., Anasooya Shaji, C. & Nixon, K. Neuroimmune Activation and Microglia Reactivity in Female Rats Following Alcohol Dependence. *Int J Mol Sci* **25**, doi:10.3390/ijms25031603 (2024).
48 Marshall, S. A., McClain, J. A., Wooden, J. I. & Nixon, K. Microglia Dystrophy Following Binge-Like Alcohol Exposure in Adolescent and Adult Male Rats. *Front Neuroanat* **14**, 52, doi:10.3389/fnana.2020.00052 (2020).
49 Peng, H., Geil Nickell, C. R., Chen, K. Y., McClain, J. A. & Nixon, K. Increased expression of M1 and M2 phenotypic markers in isolated microglia after four-day binge alcohol exposure in male rats. *Alcohol* **62**, 29-40, doi:10.1016/j.alcohol.2017.02.175 (2017).
50 Warden, A. S. *et al.* Microglia Control Escalation of Drinking in Alcohol-Dependent Mice: Genomic and Synaptic Drivers. *Biol Psychiatry* **88**, 910-921, doi:10.1016/j.biopsych.2020.05.011 (2020).
51 Nelson, J. C., Greengrove, E., Nwachukwu, K. N., Grifasi, I. R. & Marshall, S. A. Repetitive binge-like consumption based on the Drinking-in-the-Dark model alters the microglial population in the mouse hippocampus. *J Integr Neurosci* **20**, 933-943, doi:10.31083/j.jin2004094 (2021).
52 Marsland, P. *et al.* Sex-specific effects of ethanol consumption in older Fischer 344 rats on microglial dynamics and Abeta((1-42)) accumulation. *Alcohol* **107**, 108-118, doi:10.1016/j.alcohol.2022.08.013 (2023).
53 Salem, N. A. *et al.* Cell-type brain-region specific changes in prefrontal cortex of a mouse model of alcohol dependence. *Neurobiol Dis* **190**, 106361, doi:10.1016/j.nbd.2023.106361 (2024).
54 Schrank, S. *et al.* Binge ethanol consumption can be attenuated by systemic administration of minocycline and is associated with enhanced neuroinflammation in the central amygdala. *Neuropharmacology* **262**, 110174, doi:10.1016/j.neuropharm.2024.110174 (2024).
55 Bull, C. *et al.* Rat nucleus accumbens core astrocytes modulate reward and the motivation to self-administer ethanol after abstinence. *Neuropsychopharmacology* **39**, 2835-2845, doi:10.1038/npp.2014.135 (2014).
56 Erickson, E. K., Farris, S. P., Blednov, Y. A., Mayfield, R. D. & Harris, R. A. Astrocyte-specific transcriptome responses to chronic ethanol consumption. *Pharmacogenomics J* **18**, 578-589, doi:10.1038/s41397-017-0012-2 (2018).
57 Nentwig, T. B. *et al.* Central Amygdala Astrocyte Plasticity Underlies GABAergic Dysregulation in Ethanol Dependence. *bioRxiv*, doi:10.1101/2024.06.11.598470 (2024).
58 Sriji, S. N., Akhtar, N. & Mallick, H. N. Mediodorsal thalamus lesion increases paradoxical sleep in rats. *Sleep Sci* **14**, 33-38, doi:10.5935/1984-0063.20190155 (2021).
59 Schreiner, T., Kaufmann, E., Noachtar, S., Mehrkens, J. H. & Staudigl, T. The human thalamus orchestrates neocortical oscillations during NREM sleep. *Nat Commun* **13**, 5231, doi:10.1038/s41467-022-32840-w (2022).
60 Shin, A. *et al.* A brainstem-to-mediodorsal thalamic pathway mediates sound-induced arousal from slow-wave sleep. *Curr Biol* **33**, 875-885 e875, doi:10.1016/j.cub.2023.01.033 (2023).
61 Lusk, N., Meck, W. H. & Yin, H. H. Mediodorsal Thalamus Contributes to the Timing of Instrumental Actions. *J Neurosci* **40**, 6379-6388, doi:10.1523/JNEUROSCI.0695-20.2020 (2020).
62 Koob, G. F. & Colrain, I. M. Alcohol use disorder and sleep disturbances: a feed-forward allostatic framework. *Neuropsychopharmacology* **45**, 141-165, doi:10.1038/s41386-019-0446-0 (2020).

63 Meyrel, M., Rolland, B. & Geoffroy, P. A. Alterations in circadian rhythms following alcohol use: A systematic review. *Prog Neuropsychopharmacol Biol Psychiatry* **99**, 109831, doi:10.1016/j.pnpbp.2019.109831 (2020).
64 Perreau-Lenz, S. & Spanagel, R. Clock genes x stress x reward interactions in alcohol and substance use disorders. *Alcohol* **49**, 351-357, doi:10.1016/j.alcohol.2015.04.003 (2015).
65 Spanagel, R., Rosenwasser, A. M., Schumann, G. & Sarkar, D. K. Alcohol consumption and the body's biological clock. *Alcohol Clin Exp Res* **29**, 1550-1557, doi:10.1097/01.alc.0000175074.70807.fd (2005).
66 Davis, B. T. t., Voigt, R. M., Shaikh, M., Forsyth, C. B. & Keshavarzian, A. Circadian Mechanisms in Alcohol Use Disorder and Tissue Injury. *Alcohol Clin Exp Res* **42**, 668-677, doi:10.1111/acer.13612 (2018).